ASVMR: Adaptive SVM-Based Routing Protocol in the Underwater Acoustic Sensor Network for Smart Ocean

Shuyun Zhang , Huifang Chen * , Lei Xie

Posted Date: 14 August 2023

doi: 10.20944/preprints202308.0939.v1

Keywords: Underwater acoustic sensor network (UASN); intelligent routing protocol; support vector machine (SVM); packet delivery ratio (PDR)

Article

ASVMR: Adaptive SVM-Based Routing Protocol in the Underwater Acoustic Sensor Network for Smart Ocean

Shuyun Zhang [1], Huifang Chen [1,2,3,*] and Lei Xie [1,2]

[1] College of Information Science and Electronic Engineering, Zhejiang University, Hangzhou 310027, China
[2] Zhejiang Provincial Key Laboratory of Information Processing, Communication and Networking, Hangzhou 310027, China
[3] Zhoushan Ocean Research Center, Zhejiang University, Zhoushan 316021, China
* Correspondence: chenhf@zju.edu.cn

Abstract: Underwater acoustic sensor network (UASN) plays a crucial role in collecting real-time data from remote areas of the ocean. However, deploying the UASN is a challenging problem due to the harsh environment and high deployment cost. Therefore, it is essential to design an appropriate routing protocol to effectively address the issues of routing void, packet delivery delay, and energy utilization. In this paper, an adaptive support-vector-machine-based routing (ASVMR) protocol is proposed for the UASN to prolong the network lifetime and reduce the end-to-end packet delivery delay. The proposed protocol employs a distributed routing approach that dynamically optimizes the routing path in real-time by considering four types of node state information. Moreover, the ASVMR protocol establishes a "routing vector" spanning from the current node to the sink node, and selects a suitable pipe radius according to the packet delivery ratio (PDR). In addition, the ASVMR protocol incorporates future states of sensor nodes into the decision-making process, along with the adoption of a waiting time mechanism and routing void recovery mechanism. Extensive simulation results demonstrate that the proposed ASVMR protocol performs well, in terms of the PDR, the hop count, the end-to-end delay, and the energy efficiency in dynamic underwater environments.

Keywords: Underwater acoustic sensor network (UASN); intelligent routing protocol; support vector machine (SVM); packet delivery ratio (PDR)

1. Introduction

The ocean covers more than 70% of the Earth's surface, and provides valuable services to both humans and the environment, which makes the ocean monitor becoming crucial. Therefore, advanced technologies are required to monitor the assets effectively. In this regard, remote sensing provides an excellent opportunity to study various oceanographic parameters using archived, consistent, and multitemporal datasets in a cost-efficient approach [1,2]. However, traditional ocean remote sensing technologies are limited by several factors, such as weather, the limited coverage of sensing devices, and unreliable data transmission. In recent years, the underwater internet of things (UIoT), which can obtain real-time ocean data and transmit it to the shore for further analysis and processing, is regarded as a new paradigm of ocean remote sensing.

Figure 1 illustrates the basic schematic of the UIoT, encompassing various modules for underwater sensing and transmission (underwater sensor nodes and surface nodes), underwater computing and transmission [autonomous underwater vehicles (AUVs)], surface computing and transmission [surface base station (BS), surface ships, and surface nodes], as well as coastal control (seashore BS and seashore control center) [3–5].

As critical infrastructure in the UIoT, underwater acoustic sensor network (UASN) collects data from remote areas of the ocean in real-time, enabling the acquisition of rich and accurate ocean data [6]. By deploying numerous sensor nodes under water, the UASN plays a crucial role in improving

Preprints (www.preprints.org) | NOT PEER-REVIEWED | Posted: 14 August 2023 doi:10.20944/preprints202308.0939.v1

remote sensing capability, understanding the complex dynamics of the ocean, and assessing the impact on the environment.

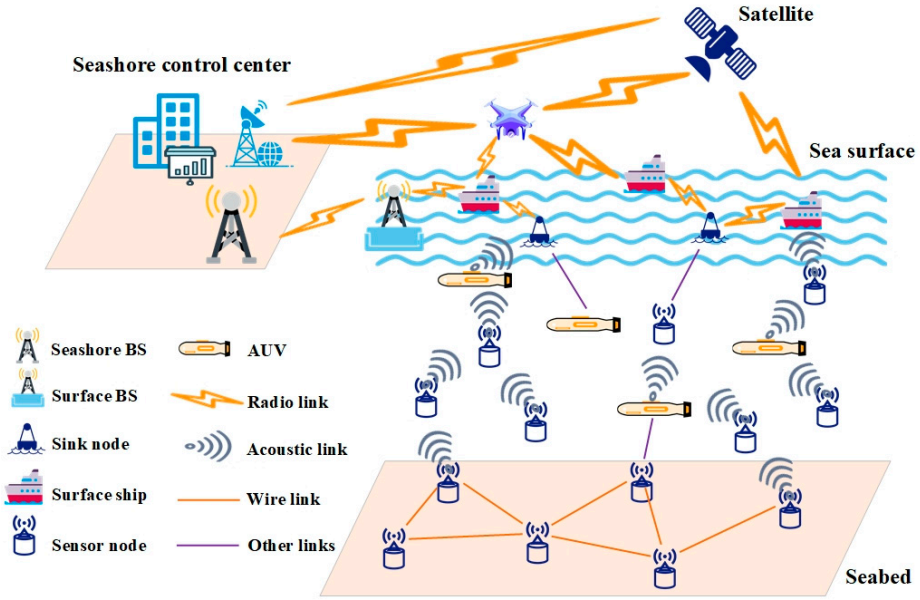

Figure 1. The schematic of the underwater internet of things.

Due to the harsh environment and high deployment cost, deploying the UASN is challenging. First, the sound signal propagates much slowly in the water at approximately 1500 m/s, resulting in a significant propagation latency. Second, some factors, such as water absorption, scattering, and underwater noise interference, limit the data transmission rate of underwater acoustic signal. Third, the complexity and uncertainty of the underwater environment further increase the difficulty of underwater acoustic communication. Hence, underwater sensor nodes consume much more energy than the terrestrial counterparts when transmitting data of the same size [7]. To maximize energy utilization and data transmission efficiency in the UASN, it is crucial to design an appropriate routing protocol which can be flexibly employed in the dynamic underwater environment.

Over the past decade, many routing protocols tailored specifically for the UASN have been proposed [8–10]. Traditional routing protocols [11–18], which are typically based on fixed routing table or static network topology, are not suitable for the UASN due to the dynamic nature of the underwater environment and the limitations of underwater acoustic signal transmission. The use of traditional routing protocols in the UASN can result in significant propagation latency, data transmission rate limitations, and increased energy consumption in underwater sensor nodes. These limitations bring about the routing void, the long packet delay, and data packet loss, which can significantly degrade the network performance. In general, there are two types of traditional routing protocols in the UASN, namely the location-aware routing protocol [11–14] and the depth-aware routing protocol [15–18].

For the location-aware routing protocol, it is assumed that sensor nodes have the knowledge of the location information with the assistance of the node positioning technology. In the vector-based forwarding (VBF) protocol proposed in [11], data packets are forwarded in a virtual pipeline with a pre-defined radius. The virtual pipeline is specified by the routing vector from the location of the source node to the destination. For the dense network, the VBF protocol effectively controls the size of the network flooding area in dense networks. However, in spare networks, the VBF protocol exhibits poor performance and fails to address routing voids. Hence, an enhanced VBF protocol, named hop-by-hop vector-based forwarding (HH-VBF), was proposed in [12]. In the HH-VBF protocol, the concept of the virtual routing pipe is adopted, where per hop virtual pipe for each forwarder is used, and each intermediate node makes decision about the pipe direction according to the current location. Hence, although the number of neighboring nodes is small, the HH-VBF protocol

 doi:10.20944/preprints202308.0939.v1

can still find a data delivery path as long as a sensor node is available in the forwarding path within the communication range. However, the hop-by-hop nature introduces much more signaling overhead for the HH-VBF protocol. In [13], a geographic routing protocol and two topology control algorithms were proposed based on the greedy forwarding protocol. When data packet is transmitted to the void node, the node can move vertically to connect with non-void nodes and recover the data forwarding. However, the location adjustment of sensor nodes requires a significant amount of energy. For demonstrated decent performance, these algorithms need an accurate 3-D location information of sensor nodes which is difficult to obtain in the UASN [14].

For the depth-aware routing protocol, only the depth information which can be obtained by the barometer on the sensor node is used to make the routing decision. The depth-based routing (DBR) protocol, the first routing solution exploiting the depth of sensor node to forward data in the UASN, was proposed in [15]. Moreover, a holding time mechanism is designed to help coordinate the transmission of forwarding candidates. However, in a sparse network, the greedy hop-by-hop forwarding may frequently access a communication void region, where the sensor node cannot find a next-hop node to deliver the data packet. The energy-efficient depth-based routing (EE-DBR) protocol, where both the residual energy and the depth of sensor nodes are considered for selecting the next-hop node, was proposed in [16]. However, when sensor nodes are deployed sparsely, the problem of the routing void was not resolved effectively. In [17], the distance-vector-based opportunistic routing (DVOR) protocol was proposed. The DVOR protocol seeks the shortest routing path according to the hop count of sensor nodes towards the destination. Additionally, a holding time mechanism is developed to schedule data packet forwarding. However, the DVOR protocol uses the periodic beacons to dynamically establish the routing path, which results in overhead for the UASN. In [18], the adaptive power-controlled depth-based routing protocol (APCDBRP) was proposed to prolong the network lifetime. The protocol comprises two phases: route establishment and data transmission. Moreover, APCDBRP proposes a data protection and route reconstruction mechanism to address issues such as network topology changes. However, the power control and data protection mechanisms in APCDBRP introduce a certain level of end-to-end delay. The depth-based routing methods use the greedy algorithm to forward data packets, where sensor nodes passively receive data packets. Although some methods have been used to limit the redundancy, the area around the forwarding nodes is still subject to flooding, resulting in the energy waste. Additionally, due to the acoustic communication between underwater sensor nodes, the transmission rate is limited, and excessive packet transmission in the network easily leads to the failure of important packet forwarding.

With the development of artificial intelligence (AI), increasingly complex AI technologies are being used to design routing protocol [19]. Intelligent routing protocols [20–23] have been proposed to address the challenges faced by traditional routing protocols in the UASN. These protocols can dynamically adapt to changes in the network environment, select the optimal path based on real-time monitoring of network status and node changes, and optimize the energy consumption to reduce routing void, minimize the packet delivery delay, and prolong the network lifespan. In addition, intelligent routing protocols enhance the network security by selecting more secure path.

In [20], an ant colony optimization algorithm (ACOA) and artificial fish swarm algorithm (AFSA) fusion algorithm was proposed for the routing protocol in the UASN. An adaptive mechanism is used to combine the advantages of ACOA and AFSA. The method first uses the AFSA to calculate a set of globally optimal paths. To address the problem of insufficient precision in the optimal path calculation of the AFSA, a parallel ACOA is then employed to select the optimal path. However, the method is not suitable for resource-limited underwater nodes due to the high computation complexity. In [21], a Q-learning-based localization-free anypath routing (QLFR) protocol was proposed, where the Q-value is calculated by jointly considering the residual energy and the depth of sensor nodes. In addition, a new holding time mechanism for data packet forwarding is designed according to the priority of forwarding candidate nodes. Nevertheless, the intricate mechanism and substantial computation demand involved pose challenge for implementing in the underwater environment. In [22], a reinforcement learning-based opportunistic routing

Preprints (www.preprints.org) | NOT PEER-REVIEWED | Posted: 14 August 2023 doi:10.20944/preprints202308.0939.v1

(RLOR) protocol was proposed by combining the advantages of opportunistic routing algorithm and reinforcement learning algorithm. In addition, a recovery mechanism is employed in the RLOR protocol to enable the data packet to bypass the void area efficiently and continue to forward, and the packet delivery ratio (PDR) is improved in the sparse network. However, the RLOR protocol uses the specified value combination which cannot be adaptively adjusted according to the change of environment. In [23], the deep Q-network (DQN)-based energy and latency-aware routing (DQELR) protocol was proposed. The DQELR protocol uses DQN to train agents since the Q-learning-based methods are not suitable for environments with a large state space. Each data packet is defined as an agent, and the depth and residual energy are considered to design the reward function. The DQELR protocol can extend the network lifetime, as well as satisfying the energy consumption and latency constraints. However, the additional cost resulting from Q-learning-related information exchange is not addressed.

The routing methods mentioned above improve the efficiency of data transmission and reduce energy consumption to some extent. However, the issues of high packet loss rate and long end-to-end delay are not be addressed effectively. Furthermore, these methods lack the ability to adjust in real-time and recover the forwarding process when data packets become trapped in routing voids. To address these issues, an adaptive support-vector-machine-based routing (ASVMR) protocol is proposed for the UASN. In the proposed ASVM routing protocol, SVM is utilized to train the model for selecting the relay node, where four factors are selected as features for the model. A reasonable routing pipe radius is chosen based on the PDR to minimize latency and extend the network lifetime. Moreover, a waiting time mechanism is design for the opportunity routing to improve the PDR. To deal with the transmission failure of the routing void, each sensor node can activate the recovery mechanism to bypass the void region and continue forwarding data packets. To the best of our knowledge, this work is the first attempt to adopt the SVM model to design the routing protocol in the UASN. The main contributions of the paper are summarized as follows.

1. Unlike the traditional routing protocols which select the rely node with a single parameter [12,15,24], the proposed ASVMR protocol selects a set of forwarding candidates from neighboring nodes based on four factors, guaranteeing the optimal routing choice and enhancing the performance significantly.
2. The waiting time mechanism for opportunity routing is enhanced by incorporating the distance between sensor nodes, which reduces the end-to-end delay and data packet loss.
3. An adaptive routing pipe radius scheme is proposed to further reduce unnecessary transmissions, as well as maintaining a high PDR.

The remainder of the paper is organized as follows. Section 2 is the preliminaries, including the acoustic propagation model, the network model, and the SVM model. Section 3 presents the proposed ASVMR protocol in detail, and Section 4 elaborates on the design of corresponding routing protocol. The simulation results and discussions are given in Section 5. Finally, Section 6 concludes the paper.

2. Preliminaries

In this section, the acoustic propagation model, the network model, the SVM model are introduced.

2.1. Acoustic Propagation Model

Here, the Thorp model [25] is adopted for the underwater acoustic channel.

The attenuation of underwater acoustic signal with frequency f (in kHz) at transmission distance l (in meter) is given by

$$A(l,f) = l^k a(f)^l, \tag{1}$$

where, k represents the spreading coefficient, $a(f)$ is the absorption coefficient, and

$$10\log a(f) = 0.11\frac{f^2}{1+f^2} + 44\frac{f^2}{4100+f^2} + 2.75\times 10^{-4} f^2 + 0.003. \tag{2}$$

Preprints (www.preprints.org) | NOT PEER-REVIEWED | Posted: 14 August 2023 doi:10.20944/preprints202308.0939.v1

The energy consumed by the sensor node for transmitting a data packet of m-bit to the sensor node at distance l ($l < l_{\max}$) is

$$E_{\mathrm{t}}(m,l) = mP_0A(l,f), (E_{\mathrm{t}} < E_{\mathrm{remain}}), \tag{3}$$

where, P_0 represents the minimum power required for the node to send data, $l_{\max}$ denotes the maximum communication distance of sensor node, E_{remain} represents the remaining energy of sensor node, and E_{remain} is the upper limit of E_{t}.

Similarly, the energy consumed by the sensor node to receive a data packet of m-bit is

$$E_{\mathrm{r}}(m) = mP_{\mathrm{r}}, \tag{4}$$

where, P_{r} represents the reception coefficient.

Using the attenuation $A(l,f)$ can evaluate the signal noise ratio (SNR) observed at a receiver over a distance l when the transmitted signal is a tone of frequency f. Neglecting the directivity indices and losses other than the path loss, the narrow-band SNR is given by

$$SNR(l) = \frac{E_{\mathrm{b}}/A(l,f)}{N_0}, \tag{5}$$

where, E_{b} represents the average energy consumed to transmit one-bit data, and N_0 represents the noise power spectral density under the condition of additive white Gaussian noise (AWGN) channel.

In this paper, binary phase shift keying (BPSK) modulation technology [26] is considered to analyze the bit error rate. If the length of propagation distance is l, the bit error rate is

$$p_{\mathrm{e}}(l) = \frac{1}{2}\left(1 - \sqrt{\frac{SNR(l)}{1+SNR(l)}}\right). \tag{6}$$

Therefore, the probability of successful transmission of m-bit data is

$$p(m,l) = [1 - p_{\mathrm{e}}(l)]^m. \tag{7}$$

2.2. Network Model

In this paper, a network architecture with multiple sink nodes [17], as depicted in Figure 2, is considered, which simplifies the practical scenario of the UASN. The network consists of a set of sensor nodes with a maximum transmission range of R, $\mathcal{N} = \mathcal{SN} \cup \mathcal{SK}$, where $\mathcal{SN}$ denotes the set of underwater sensor nodes, and $\mathcal{SK}$ represents the set of sink nodes.

In Figure 2, the sensor nodes deployed randomly in a 3-D underwater area are equipped with acoustic modems and sensing devices to carry out observing and exploring tasks. Meanwhile, the sink nodes deployed on the water surface are equipped with both acoustic and radio-frequency (RF) modems. The acoustic modem is used for the underwater communication, which includes the communication between underwater sensor nodes, and the communication between underwater sensor nodes and sink nodes. The RF modem is used for the surface communication, which includes the communication between sink nodes, and the communication between sink nodes and satellites. The underwater sensor nodes collect data from monitoring areas, and transmit the data to sink nodes which are considered as the destinations of underwater data packets. The sink nodes aggregate the sensory data and transmit to seashore control center for further processing and analysis by satellites.

Here, we assume that a data packet is delivered successfully as it arrives at any sink node.

Preprints (www.preprints.org) | NOT PEER-REVIEWED | Posted: 14 August 2023 doi:10.20944/preprints202308.0939.v1

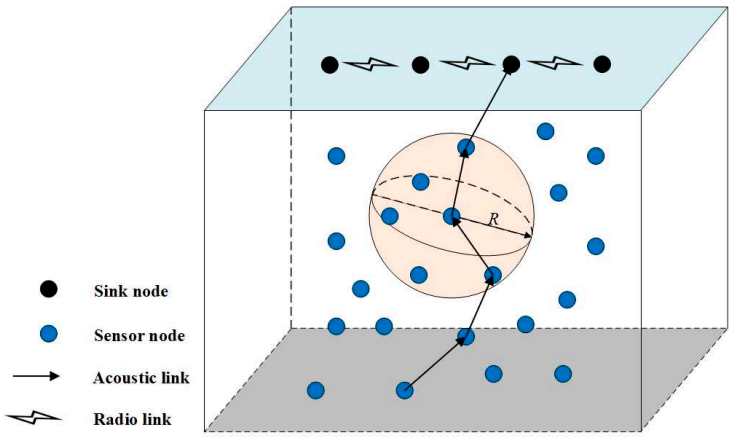

Figure 2. A network architecture of the UASN with multiple sink nodes.

2.3. SVM Model

SVM, a machine learning method based on the statistical learning theory [27], can handle high-dimensional data, solve non-linear problems, exhibit excellent generalization ability, and achieve high accuracy.

The core idea of the SVM model is to use a kernel function that satisfies the Mercer condition to replace a non-linear mapping. Hence, the sample points in the input space can be mapped to a high-dimensional feature space to facilitate linear separation, and an optimal hyperplane is constructed to approximate the ideal classification result. Hence, the SVM model is specifically used for small data samples, and is a learning machine with optimal classification and generalization capability.

Given a set of training data samples, $\mathcal{F} = \{(x_1, y_1), (x_2, y_2), \cdots, (x_n, y_n)\}$, where, $y_i \in \{-1,1\}$, the hyperplane can be expressed as

$$\omega^T x + b = 0. \tag{8}$$

If the hyperplane (ω, b) can correctly classify the training data samples, we have

$$\begin{cases} \omega^T x_i + b \geq 1, & y_i = 1, \\ \omega^T x_i + b \leq -1, & y_i = -1. \end{cases} \tag{9}$$

An optimization problem supporting the vector machine model can be constructed as

$$\begin{aligned} &\min_{\omega,b} \frac{1}{2}\|\omega\|^2 + C\sum_{i=1}^{n} \xi_i, \\ &\text{s.t. } y_i(\omega^T x_i + b) \geq 1 - \xi_i, \ i = 1,2,\cdots,n. \end{aligned} \tag{10}$$

where, ξ_i represents the degree of misclassification for sample i. In order to control the degree of misclassification, an error penalty factor C, is introduced.

As a convex quadratic programming problem, the problem formulated in (10) can be solved by transforming to the dual problem using the Lagrange multiplier method. That is,

$$L(\omega, b, \xi, \alpha, \beta) = \frac{1}{2}\|\omega\|^2 + C\sum_{i=1}^{n}\xi_i - \sum_{i=1}^{n}\alpha_i \times \left[y_i(\omega x_i + b) - 1 + \xi_i\right] - \sum_{i=1}^{n}\beta_i\xi_i, \tag{11}$$

where, α_i and β_i are Lagrange multipliers, $\alpha_i \geq 0$ and $\beta_i \geq 0$.

The dual problem of (11) is obtained as

Preprints (www.preprints.org) | NOT PEER-REVIEWED | Posted: 14 August 2023 doi:10.20944/preprints202308.0939.v1

$$\max_{\alpha} \sum_{i=1}^{n} \alpha_i - \frac{1}{2} \sum_{i=1}^{n} \sum_{j=1}^{n} \alpha_i \alpha_j y_i y_j k(x_i, x_j),$$
$$\text{s.t.} \sum_{i=1}^{n} \alpha_i y_i = 0, 0 \le \alpha_i \le C, i = 1,2,\cdots,n. \tag{12}$$

The decision function can be defined as

$$f(x) = \omega^T x + b = \sum_{i=1}^{n} \alpha_i y_i k(x_i, x) + b, \tag{13}$$

where, $k(\cdot, \cdot)$, the kernel function, can be a linear function, a polynomial function, or a radial basis function (RBF).

3. Proposed ASVMR Protocol

In this section, the proposed ASVMR protocol is presented in detail. The framework of SVM adapted for routing is first introduced. And then, a detailed description of the proposed ASVMR protocol, including the determination of next hop, the dynamic timer, the adaptive pipe radius scheme and the recovery mechanism, is presented.

3.1. The Framework of SVM

To minimize latency and prolong the network lifetime, four factors, namely the ratio of depth difference and the maximum communication range, the ratio of depth difference and the distance of sensor nodes, the residual energy function and the neighboring node function, are selected as features for training the SVM model for routing. These factors collectively form a four-dimensional sample, represented by x_k.

Suppose that node n_i sends a data packet to node n_j, (x_i, y_i, z_i) and (x_j, y_j, z_j) represent the positions of nodes n_i and n_j, respectively. The ratio of depth difference and the maximum communication range R can be defined as

$$drRatio(n_i, n_j) = \frac{z_j - z_i}{R}. \tag{14}$$

The ratio of depth difference and the distance between nodes n_i and n_j can be defined as

$$ddRatio(n_i, n_j) = \frac{z_j - z_i}{\sqrt{(x_j - x_i)^2 + (y_j - y_i)^2 + (z_j - z_i)^2}}. \tag{15}$$

The residual energy function at node n_j can be defined as

$$f_e(n_j) = \frac{e_{\text{res}}(n_j)}{e_{\text{ini}}(n_j)}, \tag{16}$$

where, $e_{\text{ini}}(n_j)$ and $e_{\text{res}}(n_j)$ denote the initial and residual energy of node n_j, respectively.

The neighboring node function at node n_j can be defined as

Preprints (www.preprints.org) | NOT PEER-REVIEWED | Posted: 14 August 2023 doi:10.20944/preprints202308.0939.v1

$$f_{\mathrm{n}}(n_j) = \frac{nei(n_j)}{nei_{\max}}, \tag{17}$$

where, $nei(n_j)$ represents the number of neighboring nodes of node n_j, and $nei_{\max}$ is the maximum number of neighboring nodes among all sensor nodes in the network.

Therefore, the sample k can be expressed as $x_k = \{drRatio, ddRatio, f_{\mathrm{e}}, f_{\mathrm{n}}\}$.

Here, we employed a portion of the publicly available ASUNA dataset [28] consisting in 11000 sample groups including 6561 positive and 4439 negative samples. A partial training samples are listed in Table 1.

Table 1. Partial training samples.

$drRatio$ $x_1 \in (0, 1]$	$ddRatio$ $x_2 \in (0, 1]$	f_{e} $x_3 \in (0, 1]$	f_{n} $x_4 \in [0, 1]$	$label$ $y \in \{-1, 1\}$
0.6	0.6	0.9	0	-1
0.2	0.1	0.7	0.6	-1
0.7	0.4	0.5	0.2	1
0.4	0.8	0.4	0.4	1

Here, the value of $drRatio$, $ddRatio$ and f_{e} is set within (0, 1], and value of f_{n} is set within [0, 1]. The value of y is determined based on the result provided by ASUNA and manual judgment. For example, in the first sample of Table 1, the node has no neighboring nodes with $x_4 = 0$, and thus, the label y is set to –1. We randomly selected 2500 samples for training the model, normalized them and employed 5-fold cross-validation with an RBF kernel function. The test accuracy achieves 99.988%.

3.2. The Determination of Next Hop

We comprehensively consider the node depth and the pipe radius of the routing vector to select the candidate forwarding set from the set of neighboring nodes. The set of sensor nodes in the UASN is defined as $\mathcal{SN} = \{n_1, n_2, \cdots, n_m\}$, where, m is the number of sensor nodes.

First, sensor nodes in the routing vector and above node n_i are grouped into the candidate forwarding set of node n_i. The schematic diagram depicting the candidate forwarding set selection is illustrated in Figure 3, where, $\mathcal{N}_{\mathrm{nei},i}(t)$ denotes the set of neighboring nodes of node n_i at time t, $\mathcal{S}_{\mathrm{above},i}(t)$ represents the candidate forwarding set selected for node n_i at time t. The shaded rectangle is the routing pipe.

Second, node n_i acquires the state values of sensor nodes in the candidate forwarding set and incorporates these values into the SVM model to obtain the one-hop decision value v_t at time t, in (13). In order to reflect the influence of future states on the current state, the decision value at time t is defined as

$$V_t = v_t + \gamma v_{t+1} + \gamma^2 v_{t+2} + \cdots = \sum_{i=0}^{\infty} \gamma^i v_{t+i}. \tag{18}$$

where, γ denotes the discount factor.

Preprints (www.preprints.org) | NOT PEER-REVIEWED | Posted: 14 August 2023 doi:10.20944/preprints202308.0939.v1

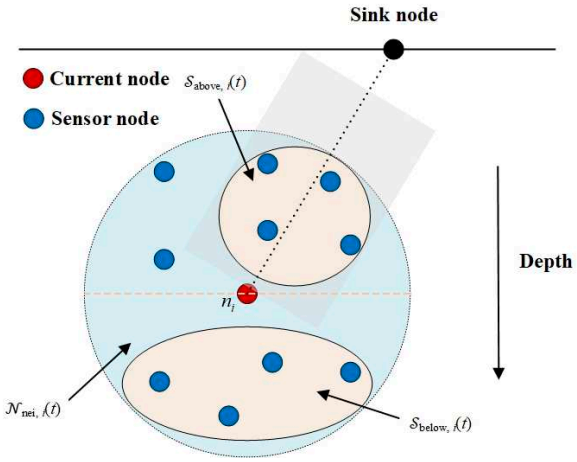

Figure 3. The Schematic diagram of candidate forwarding set selection.

To reduce the computational complexity, we only compute the value V_t for γ raised to the first power, and the node with maximum value of V_t is chosen as the next hop. It is worth noticing that the four factors of a node are constantly changing due to the continuous movement underwater and energy depletion. Therefore, V_t varies with time t, and the latest feature space information is utilized for each calculation of V_t.

3.3. A Dynamic Timer

The preceding section primarily focuses on selecting the most suitable next-hop node. However, in underwater environments, communication via single-path transmission is unreliable. To enhance the PDR, this model adopts an opportunistic routing approach to forward packets once the optimal next-hop node has been identified. Furthermore, a dynamic timer is employed to correlate the waiting time with the distance between the current node and the optimal next-hop node, ensuring that data packets can be transmitted to the previously selected optimal next-hop node.

Opportunistic routing involves a node initially forwarding data packets to a group of candidate nodes, each of which retains a copy of data packets [29]. Subsequently, each candidate node can set its own timer to determine how long it will keep the copy. Once a timer expires, the corresponding node is designated as the relay node, and other candidates can observe this behavior and discard their copies. This mechanism enhances data transmission reliability, reduces redundant transmission, and conserves energy. However, the timer in this process increases the end-to-end delay.

To further decrease the end-to-end delay, an adaptive timer setting based on node distance is addressed in this paper. Specifically, closer nodes have shorter waiting times, allowing them to forward data packets more swiftly and reducing the end-to-end delay.

Figure 4 depicts a scenario where node n_i has a set of neighboring nodes, where node n_j having the maximum decision value. In this case, node n_i selects node n_j as the next-hop node and transmits the data packet to it, along with the ID and position of node n_j. Upon receiving the packet, node n_j immediately forwards it while other nodes store a copy and calculate their distance from node n_j. If this distance is less than the maximum communication range R, the node sets a timer. If a forwarding packet from node n_j is not received before the timer expires, it forwards the stored replica in the hope of reaching node n_j. The variable W represents the routing pipe radius, and the number of sensor nodes in the candidate forwarding set can be adjusted according to the routing pipe radius. The maximum value of W is R.

Assuming that node n_k is within the maximum communication range of both node n_i and node n_j, the waiting time of node n_k can be constructed as

$$T_{\text{wait}}(k) = \frac{d_{ij}+d_{jk}-d_{ik}}{v} + rand(0, \frac{R}{v}). \tag{19}$$

Preprints (www.preprints.org) | NOT PEER-REVIEWED | Posted: 14 August 2023 doi:10.20944/preprints202308.0939.v1

where, d_{ij}, d_{jk} and d_{ik} represent the distance between node n_i and node n_j, node n_j and node n_k, node n_i and node n_k, respectively; v is the sound speed in water; function $rand(a, b)$ generates a random real number within range (a, b). In (19), the first term reflects the waiting time required for node n_k to receive the data packet from node n_i and then from node n_j. The second term represents a random waiting time set to avoid the occurrence of collisions between nodes with the same waiting time.

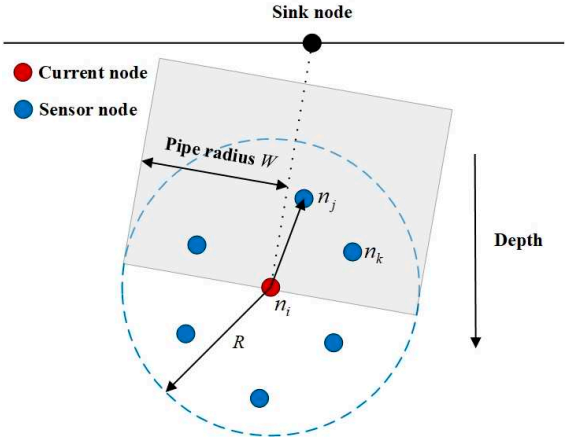

Figure 4. The schematic of the neighboring nodes of a node.

3.4. Adaptive Pipe Radius Scheme

In practice, it is typical to select a sufficiently large routing pipe radius to increase the number of candidate forwarding nodes and improve the PDR. However, a larger radius also enables more sensor nodes with comparable waiting times to forward the same data packet, which results in redundant transmissions and energy waste. To enhance energy efficiency, it is necessary to impose additional restrictions on data packet transmissions during the routing process.

However, if data packet transmissions are suppressed excessively, it will result in a reduction of the PDR, which represents the ratio of successfully received data packets to the number of generated data packets. The PDR is a measure of transmission reliability. Therefore, to enhance energy efficiency and maintain high transmission reliability, we propose an adaptive pipe radius scheme.

First, the routing pipe radius is initialized as the maximum value R, and a threshold of PDR is adopted to balance energy consumption and transmission reliability, which can be customized based on the practical application scenario of the UASN.

Second, the source attaches the number of generated data packets to the transmitted data packet during the data packet transmission phase. Upon receiving the data packet, the sink node calculates the PDR by dividing the number of successfully delivered data packets by the total number of generated data packets.

If PDR exceeds the threshold, the routing pipe radius will be reduced during the subsequent transmission to improve energy efficiency. If PDR falls below the threshold, the sink node will broadcast a message to increase the routing pipe radius, and the source will attach the new routing pipe radius to the transmitted data packet. This will result in an increase in the pipe radius of eligible forwarders during the next transmission round, which improved the delivery ratio.

The proposed adaptive pipe radius scheme is illustrated in Algorithm 1.

Algorithm 1: Adaptive Pipe Radius Scheme

R is the communication range of nodes. P_{gen} is the total number of generated data packets. P_{rec} is the number of successfully received data packets. PDR is the current packet delivery rate. PDR_{th} is the threshold of PDR for the application scenario.

1: Initialize the routing pipe radius to R

2: **while** the packet transmission phase is not completed **do**

Preprints (www.preprints.org) | NOT PEER-REVIEWED | Posted: 14 August 2023 doi:10.20944/preprints202308.0939.v1

Start a new round of data packet transmission
Attach P_{gen} to the transmitted data packet at the source
Calculate the PDR at the sink node using $PDR = \frac{P_{\text{rec}}}{P_{\text{gen}}}$
if $PDR > PDR_{\text{th}}$ **then**
    Decrease the routing pipe radius during the next transmission round
else
    Increase the routing pipe radius during the next transmission round
end if
end while

3.5. Recovery Mechanism

If the node cannot find any other neighboring nodes with a shorter distance from the sink node, a void node appears [30]. During data transmission, selecting a void node as the next hop will result in the data packet loss, which consumes the energy and reduces the data transmission efficiency. To address this issue, the proposed routing method avoids selecting void nodes in advance to trigger the recovery mode when a routing void is encountered.

First, the number of neighboring nodes is taken as a dimension in the feature space for training. The node with more neighboring nodes is more likely to be selected as the next hop. However, the method does not eliminate the routing void entirely, and some void nodes may still be chosen. Therefore, a recovery mode is incorporated that enables void nodes to locate suitable next hop for forwarding data downward, bypassing the void area effectively.

In the recovery mode, the candidate forwarding set for node n_i is composed of the nodes below and inside its pipeline, denoted as $\mathcal{S}_{\text{below},i}(t)$, as illustrated in Figure 5. Then, the next hop is determined by the value of V_t. Once the void node forwards the data packet to a non-void node, it exits the recovery mode and resumes routing data packets to the water surface. In this mode, the node records the ID of the previous hop node to prevent the routing loop.

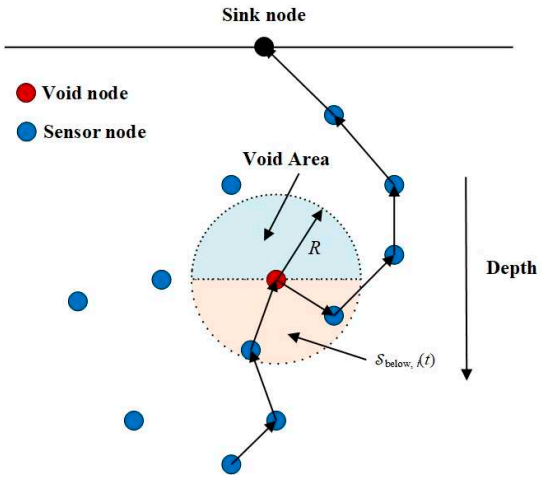

Figure 5. The schematic diagram of recovery mode.

4. The Design of Routing Protocol

In this section, a detailed design of the proposed routing protocol, including the packet structure, the exchange of node status knowledge, and the forwarding of data packets, is given.

4.1. The Packet Structure

Preprints (www.preprints.org) | NOT PEER-REVIEWED | Posted: 14 August 2023 doi:10.20944/preprints202308.0939.v1

Figure 6 illustrates the packet structure used in the network, comprising a header composed of the packet identification, the routing information, and the node status information.

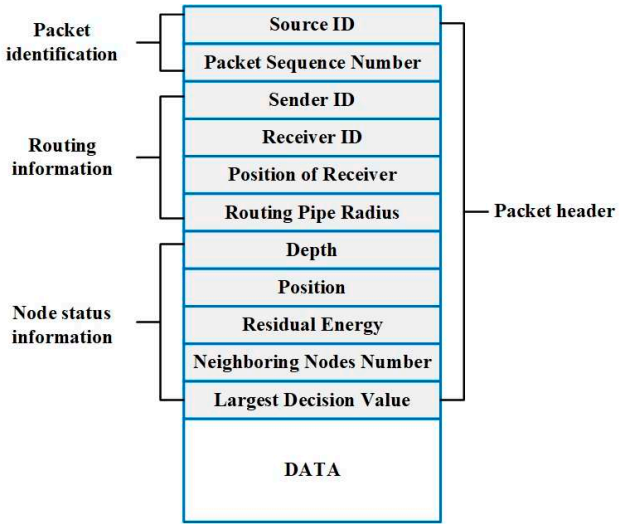

Figure 6. The structure of packet.

Packet identification fields include:

(1) Source ID, identifying the source node.
(2) Packet sequence number, providing a unique identifier for the packet.

These fields are node-specific and utilized to differentiate data packets during data forwarding, remaining constant throughout the packet's lifetime.

Routing information is used to determine the routing pipe radius, select the next hop, and assist forwarding candidates in transmitted data packets. The routing information is comprised of the following fields:

(1) Sender ID, identifying the current node.
(2) Receiver ID, identifying the optimal next hop.
(3) Position of receiver, providing the 3-D coordinates of the optimal next hop.
(4) Routing pipe radius, specifying the routing pipe radius.

The routing pipe radius size controls the number of forwarding candidates as previously discussed. The sink node determines the size through the calculation of PDR.

Each node must embed its status information in the following fields before sending a data packet.

(1) Depth, providing the depth information of the current node.
(2) Position, providing the 3-D coordinates of the current node.
(3) Residual energy, providing the remaining energy of current node.
(4) Neighboring nodes number, indicating the number of neighboring nodes of the current node.
(5) Largest decision value, providing the largest decision value among neighboring nodes of the current node.

Upon receiving a data packet, each node retrieves these fields from the packet header and updates its neighbors' information with the latest routing information, which assists them in making optimal routing decision.

In addition to the packet header, the Data field is optional. This field contains the message that should be sent to the destination. If Data is absent, the packet is used only for exchanging routing information, which will be described in the next subsection.

4.2. Node Status Knowledge Exchange

Preprints (www.preprints.org) | NOT PEER-REVIEWED | Posted: 14 August 2023 doi:10.20944/preprints202308.0939.v1

In order to make optimal routing decision, it is necessary for all sensor nodes to possess their neighboring nodes' status information to calculate decision values using an SVM model. The proposed routing protocol utilizes two methods for exchanging node status information.

- Simultaneous Exchange with Data Packet Transmission: In the proposed protocol, the status information of the sender is attached to the header of the data packet before transmission. Consequently, a node can obtain its neighboring nodes' status information from incoming data packets.
- Use of Hello Packets Containing Node Status Knowledge: Each node in the UASN periodically broadcasts a Hello packet, used solely for exchanging status knowledge. These broadcasts complement the approach of exchanging node status knowledge. Since each node can obtain neighboring node(s) status knowledge from data packet transmissions, special control packets do not need. Therefore, the broadcast period of Hello packet can be set to be long enough to eliminating the overhead.

4.3. Data Packet Forwarding

This part discusses the procedure of data packet forwarding in the proposed ASVMR protocol, as summarized in Algorithm 2.

Algorithm 2: **Data Packet Forwarding**

$Packet$ is the data packet. n_i is the node that currently receives the data packet. n_j is the receiver in the header of $Packet$. V_{n_x} is the decision value of node n_x. $\mathcal{C}_i \in \{\mathcal{S}_{\text{below},i}, \mathcal{S}_{\text{above},i}\}$ is the candidate forwarding set of n_i. d_{ij} is the distance between node n_i and node n_j. R is the communication range of n_i. $T_{\text{wait}}(i)$ is the waiting time to hold the data packet at node n_i.

On hearing $Packet$
Get the information from the header of $Packet$
if n_i has forwarded $Packet$ **then**
    Drop $Packet$
else if $n_i == n_j$ **then**
    Calculate V_{n_x} for $n_x \in \mathcal{C}_i$
    Choose the maximum V_{n_x}
    Update the header of $Packet$
    Send $Packet$ immediately
else
    Calculate d_{ij}
    if $d_{ij} > R$ **then**
        Drop $Packet$
    else
        Calculate $T_{\text{wait}}(i)$
        if n_i overhears $Packet$ during $T_{\text{wait}}(i)$ **then**
            Drop $Packet$
        else
            Update the header of $Packet$
            Send $Packet$ when $T_{\text{wait}}(i)$ expires
        end if
    end if
end if

Preprints (www.preprints.org) | NOT PEER-REVIEWED | Posted: 14 August 2023 doi:10.20944/preprints202308.0939.v1

When a sender prepares to transmit a data packet, it first checks for routing holes. If present, it enters recovery mode and forms a candidate forwarding set by selecting neighboring nodes simultaneously possessing two characteristics, namely nodes below the sender and nodes in the routing pipe. Alternatively, if routing holes are absent, a candidate forwarding set is formed by neighboring nodes simultaneously possessing two characteristics, namely nodes above the sender and nodes in the routing pipe.

Next, the sender calculates decision values associated with each candidate forwarding set using acquired status knowledge. The node with the maximum decision value is selected as the next hop and the remaining nodes in the candidate forwarding set assist in routing the data packet to the optimal next hop. The routing pipe radius controls the number of nodes in the candidate forwarding set. Before sending the data packet, the node updates the packet header with its own status information and the information of next hop.

Upon receiving a data packet, a node extracts the status knowledge of the sender from the packet header and updates the corresponding neighbor information, regardless of whether it is designated as a qualified forwarder.

Then, the node checks whether it has forwarded the data packet before. If it has, the node directly discards the data packet; otherwise, it checks whether it is the receiver. If the node is the receiver, it forwards the packet following the above procedure. If the node is not the receiver, it calculates its distance from the receiver. If the distance exceeds the communication range, the node discards the data packet. Otherwise, the node initiates a waiting time. During the waiting time, if a node overhears the same data packet, it abandons forwarding the data packet as another node has already forwarded it. If not, the node transmits the data packet when the waiting time expires.

Furthermore, the training process in the proposed method is conducted online and interactively. As mentioned earlier, during each packet transmission round, a sender calculates decision values for each candidate forwarding set using acquired status knowledge before sending a data packet.

5. Simulation Results and Discussions

The performance of the proposed ASVMR protocol is evaluated by computer simulations.

5.1. Simulation Setup

In the UASN, each sensor node in the network has a unique ID and limited energy, and is aware of the locations of sink nodes, the sender (via the packet header), one-hop neighboring nodes, and itself. Sensor nodes are distributed randomly in a 3-D area of 500m × 500m × 500m. Sensor nodes only receive information from one-hop neighboring nodes. The sink nodes with unlimited energy and the ability of communicating using RF and acoustical modes are fixed on the water surface, and act as gateways. The source nodes, which are deployed at the bottom, can move horizontally. The locations of sensor nodes are illustrated in Figure 7. The parameters in simulations are listed in Table 2.

In addition, four quantitative metrics are adopted in simulations to evaluated the performance of the proposed ASVMR protocol.

(1) The packet delivery ratio (PDR): The ratio of data packets received by the sink node to the data packets transmitted by the source node.
(2) The hop count: The average number of relay nodes required to route a data packet from the source node to the sink node.
(3) The end-to-end delay: The average time taken by a data packet sent from the source node until it is received by the sink node.
(4) The energy tax: The average energy consumed by each node to route a data packet towards the sink node.

Preprints (www.preprints.org) | NOT PEER-REVIEWED | Posted: 14 August 2023 doi:10.20944/preprints202308.0939.v1

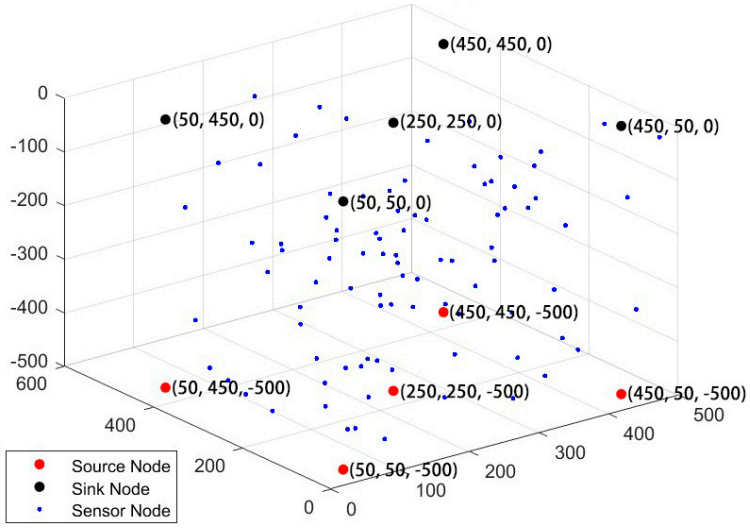

Figure 7. The placement of sensor nodes in the UASN.

Table 2. Parameters setting in simulations.

Parameter	Value
Simulation time	5000 s
The number of sink nodes	5
The number of source nodes	5
Sound speed	1500 m/s
Communication radius	150 m
Carrier frequency	25 kHz
Data generation rate	1 packet/s
Transmission rate	10 kbps
Power of transmission	2 W
Power of reception	0.1 W
Power of idle	10 mW
Number of sensor nodes	100~500
Node moving velocity	0~2 m/s
Discount factor γ	0.1~1
Routing pipe radius W	$R/8$~R

5.2. Performance Comparison

To comprehensively evaluate the performance of the proposed ASVMR protocol, three classic routing protocols are selected for comparison, namely (1) the DBR protocol [15], (2) the HH-VBF routing protocol [12], and (3) Flooding routing protocol [24]. Here, DBR and HH-VBF protocols are the representative depth-aware and location-aware routing protocols, respectively. In addition, to better demonstrate the performance of the proposed ASVMR protocol, the Flooding routing protocol in underwater networks is also included in the comparison.

First, the impact of node density on the performance of four routing protocols is simulated and compared.

Figure 8 shows the impact of node density on the performance of four routing protocols, where the node density changes as the number of sensor nodes varies from 100 to 500, the moving velocity of sensor nodes is set as 0, the discount factor is set as 0.8, and the routing pipe radius is set as R. The PDR, the hop count, the end-to-end delay, and the energy tax are shown in Figures 8(a), 8(b), 8(c), and 8(d), respectively.

Preprints (www.preprints.org) | NOT PEER-REVIEWED | Posted: 14 August 2023 doi:10.20944/preprints202308.0939.v1

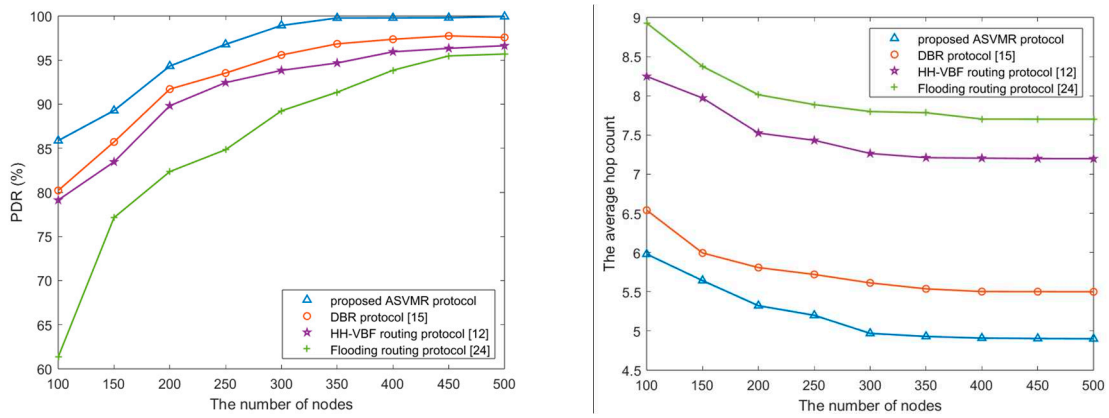

(**a**) the PDR

(**b**) the hop count

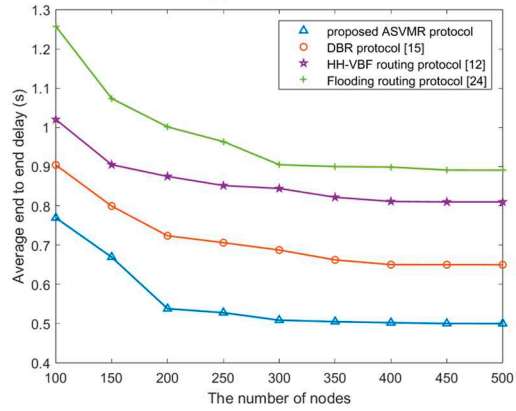

(**c**) the end-to-end delay

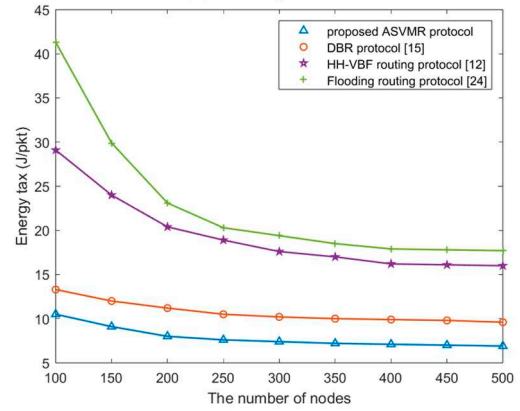

(**d**) the energy tax

Figure 8. The impact of the node density on the performance.

From Figure 8(a), we observe that as the node density increases, the PDR of four routing protocols increases gradually. This is due to the reduction in the number of void regions resulting from the deployment of nodes from sparse to dense, which allows more nodes to participate in packet forwarding and mitigates packet loss. Moreover, the proposed ASVMR protocol outperforms since it ensures the data transmission reliability through its routing pipeline and recovery mechanism.

From Figure 8(b), we observe that the hop count of four routing protocols gradually decreases as the node density increases. In a sparse network, sensor nodes may not cover the shortest path between the source and the sink node, resulting in multiple triggering of recovery mode and a high average hop count. However, in a dense network, the deployment of more nodes results in fewer void nodes and a higher probability of node coverage on the shortest path, which translates to a lower hop count. Additionally, the hop count of the proposed ASVMR protocol outperforms since it integrates an adaptive pipe radius and the SVM mechanism to identify the globally optimal next hop.

Since the hop count of the proposed ASVMR protocol performs well, it achieves low end-to-end delay and energy tax, as depicted in Figure 8(c) and Figure 8(d), respectively.

Second, the impact of node mobility on the performance of four routing protocols is simulated and compared.

Figure 9 shows the impact of node mobility on the performance of four routing protocols, where the number of sensor nodes is set as 150, the node moving velocity changes from 0 m/s to 2 m/s, the discount factor is set as 0.8, and the routing pipe radius is set as R. The PDR, the hop count, the end-to-end delay, and the energy tax are shown in Figures 9(a), 9(b), 9(c), and 9(d), respectively.

Preprints (www.preprints.org) | NOT PEER-REVIEWED | Posted: 14 August 2023 doi:10.20944/preprints202308.0939.v1

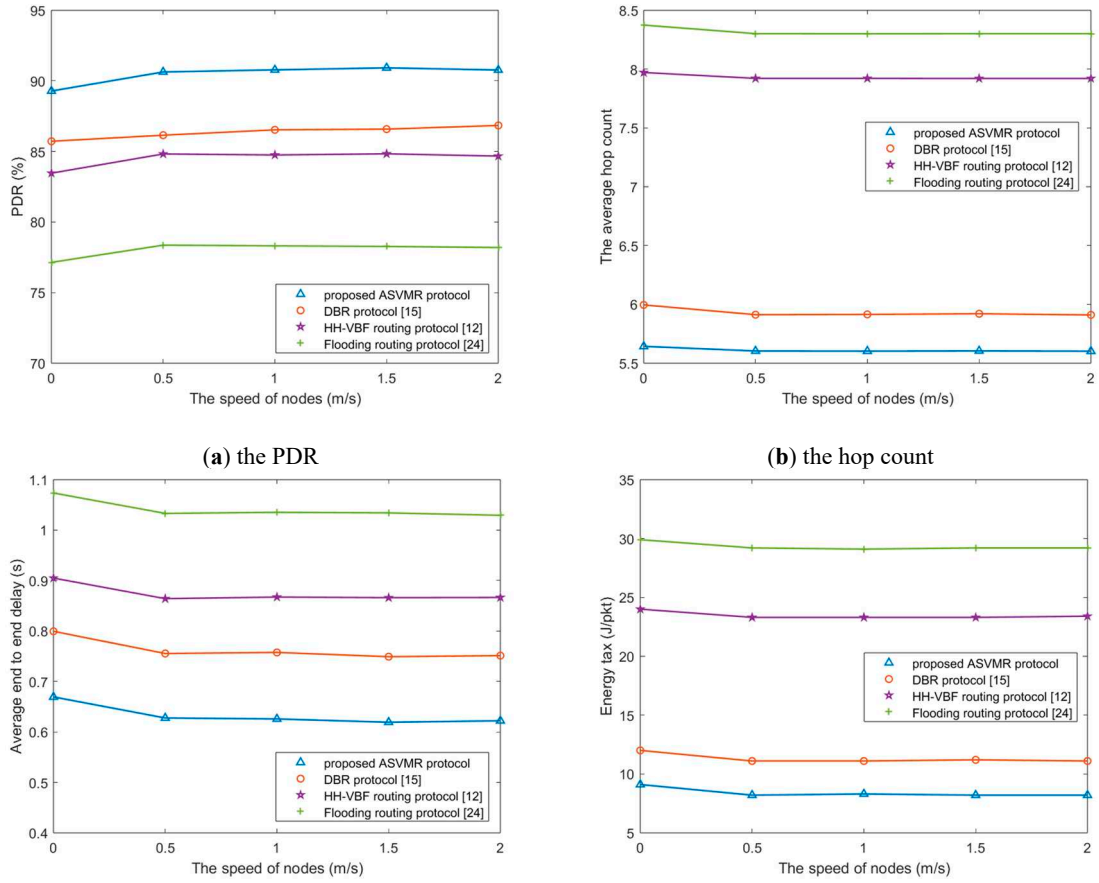

(**a**) the PDR (**b**) the hop count

(**c**) the end-to-end delay (**d**) the energy tax

Figure 9. The impact of the node mobility on the performance.

From Figure 9(a), we observe that as the node moving velocity increases, the PDR of four routing protocols increases slightly. Therefore, in a sparse network, the mobility of sensor nodes has only a slight influence on the PDR. This phenomenon occurs because the network topology changes rapidly when the node velocity increases, resulting in a fast coverage of void region. However, as the network becomes denser, the emergence of void region decreases.

From Figure 9(b), we observe that as the node moving velocity increases, the hop count of four routing protocols changes slightly. Therefore, the moving velocity of sensor nodes has a negligible influence on the hop count.

From Figure 9(c) and 9(d), we observe that the end-to-end delay and the energy tax of four routing protocols decrease slightly along with the increase of the node moving velocity. This is because the node mobility can improve network coverage, which slightly enhances the data packet transmission efficiency in the network.

Therefore, these four routing protocols can deal with the node mobility of sensor nodes effectively. Moreover, through comparison, the performance of proposed ASVMR protocol is the best, and the proposed ASVMR protocol is a suitable choice for a mobile UASN.

5.3. Impact of Parameter

First, the impact of the discount factor on the performance of the proposed ASVMR protocol is simulated.

Figure 10 shows the impact of the discount factor on the performance of the proposed ASVMR protocol, where the number of sensor nodes is set as 150, the moving velocity of sensor nodes is set as 0, the discount factor changes from 0.1 to 1, and the routing pipe radius is set as R. The PDR, the hop count, the end-to-end delay, and the energy tax are shown in Figures 10(a), 10(b), 10(c), and 10(d), respectively.

Preprints (www.preprints.org) | NOT PEER-REVIEWED | Posted: 14 August 2023 doi:10.20944/preprints202308.0939.v1

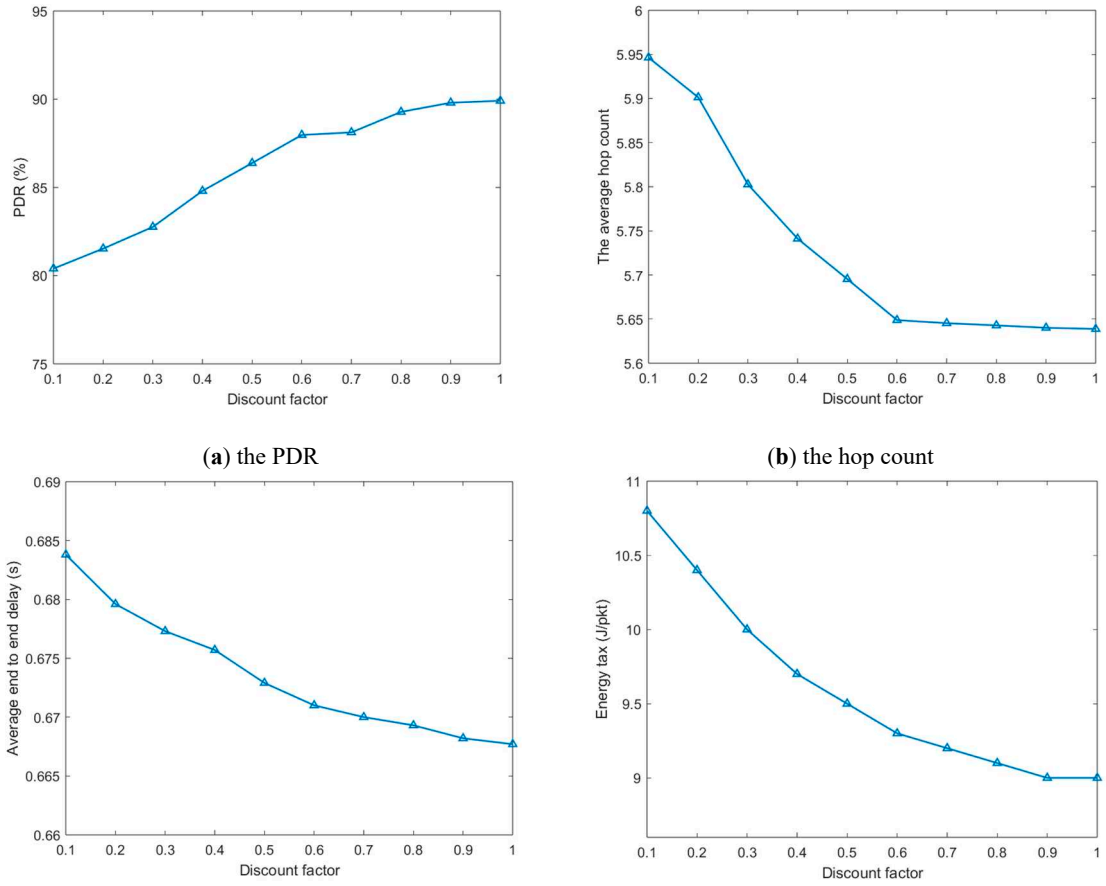

(**a**) the PDR (**b**) the hop count

(**c**) the end-to-end delay (**d**) the energy tax

Figure 10. The impact of the discount factor on the performance.

From Figure 10, we observe that the magnitude of the discount factor has a certain effect on the performance of the ASVMR protocol. As the value of the discount factor increases, the PDR increases, while the hop count, the end-to-end delay, and the energy consumption decrease.

It is demonstrated in (18) that the discount factor magnitude determines the proportion of the future one-hop decision value to the total decision value in routing decisions. A larger value of γ indicates a greater proportion of the one-hop decision value, which results in a better performance of the ASVMR protocol initially. This is because considering the future one-hop decision value in routing decision makes the decision closer to the global optimal routing than just considering the current decision value.

However, as γ further increases, the advantage becomes less apparent because the current state also affects routing decision. In general, if the computational complexity is not a main concern, incorporating all future states in the decision value calculation would benefit optimal routing decision.

Second, the impact of the routing pipe radius on the performance of the proposed ASVMR protocol is simulated.

Figure 11 shows the impact of the routing pipe radius on the performance of the proposed ASVMR protocol, where the number of sensor nodes is set as 150, the moving velocity of sensor nodes is set as 0, the discount factor is set as 0.8, and the routing pipe radius changes from $R/8$ to R. The PDR, the hop count, the end-to-end delay, and the energy tax are shown in Figures 11(a), 11(b), 11(c), and 11(d), respectively.

Preprints (www.preprints.org) | NOT PEER-REVIEWED | Posted: 14 August 2023 doi:10.20944/preprints202308.0939.v1

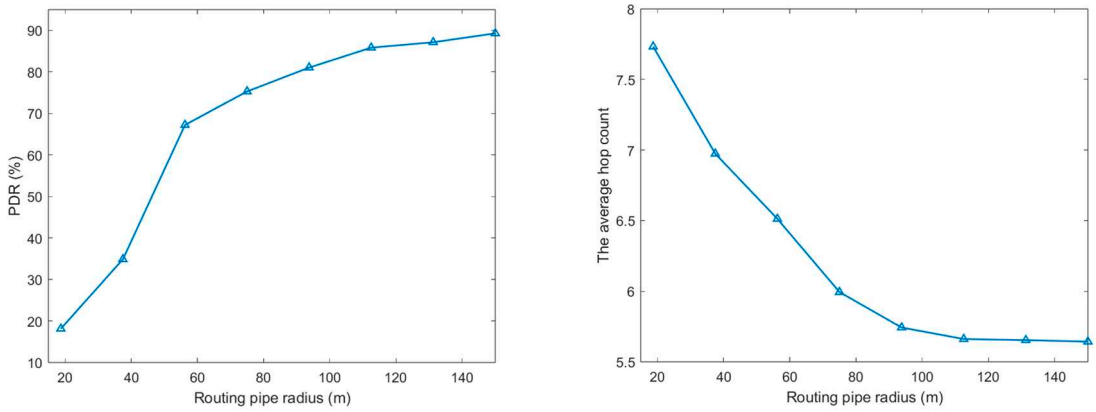

(**a**) the PDR

(**b**) the hop count

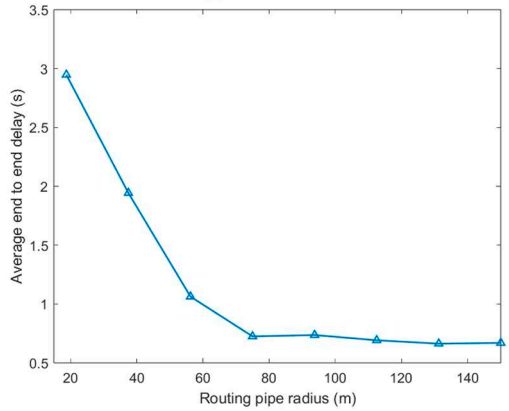

(**c**) the end-to-end delay

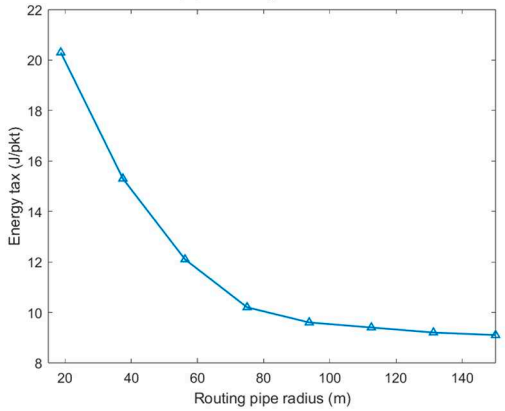

(**d**) the energy tax

Figure 11. The impact of the routing pipe radius on the performance.

From Figure 11(a), we observe that the PDR of the ASVMR protocol increases with an increase in the routing pipe radius. This is because a larger routing pipe radius can provide more neighboring nodes, which reduces routing void and lowers the packet loss rate.

From Figure 11(b), we observe that as the routing pipe radius increases, the hop count of the ASVMR protocol decreases. This is because a larger routing pipe radius can offer more nodes in the candidate forwarding set, as well as increasing the probability of finding a more optimal route.

From Figure 11(c) and Figure 11(d), we observe that as the routing pipe radius increases, the end-to-end delay and energy tax of the ASVMR protocol decrease. This is because the number of hops from the source node to the destination node decreases, resulting in a reduction in the end-to-end delay and the amount of energy consumed in each packet transmission.

Therefore, the routing pipe radius affects the performance of the ASVMR protocol significantly. The increase of the routing pipe radius results in higher PDR, smaller hop count, lower end-to-end delay and energy tax for the ASVMR protocol, which indicates that a more optimal path is selected.

6. Conclusion

In this paper, we proposed an intelligent routing protocol, the ASVMR protocol, for the UASN. In the proposed protocol, various node state information is considered to dynamically optimize routing path in real-time. Specifically, the SVM framework for routing is designed to reduce the end-to-end delay and prolong the network lifetime. The decision-making process for next hop selection incorporates the adaptive routing pipe and future states in order to reduce the energy consumption. Moreover, we introduce a waiting time mechanism and routing void recovery mechanism to improve the PDR and reduce the packet loss in dynamic underwater environments. Simulation results show that the proposed ASVMR protocol performs well, in terms of the PDR, the hop count, the end-to-end delay, and the energy tax.

In the future, other parameters in the UASN, such as the transmission rate and the link quality, would be considered to further enhance the accuracy and effectiveness of routing decision.

Supplementary Materials: None.

Author Contributions: Conceptualization, S.Z. and H.C.; methodology, S.Z. and H.C.; software, S.Z.; validation, S.Z., H.C. and L.X.; formal analysis, S.Z. and H.C.; investigation, S.Z.; resources, H.C. and L.X.; data curation, S.Z.; writing—original draft preparation, S.Z.; writing—review and editing, S.Z. and H.C.; visualization, S.Z.; supervision, H.C.; project administration, H.C. and L.X.; funding acquisition, H.C. and L.X. All authors have read and agreed to the published version of the manuscript.

Funding: This research was funded by the National Natural Science Foundation of China, grant numbers 42227901 and 62271442, the Science and Technology Department of Zhejiang Province, grant number GG22F019348, and the Natural Science Foundation of Zhejiang Province, grant number LZ23F010006.

Data Availability Statement: The data that support the findings of this study are available from the corresponding author upon reasonable request.

Conflicts of Interest: The authors declare no conflict of interest.

References

1. Amani, M.; Moghimi, A.; Mirmazloumi, S.M.; Ranjgar, B.; Ghorbanian, A.; Ojaghi, S.; Ebrahimy, H.; Naboureh, A.; Nazari, M.E.; Mahdavi, S.; et al. Ocean Remote Sensing Techniques and Applications: A Review (Part I). *Water* **2022**, *14*, 3400, doi:10.3390/w14213400.
2. Amani, M.; Mehravar, S.; Asiyabi, R.M.; Moghimi, A.; Ghorbanian, A.; Ahmadi, S.A.; Ebrahimy, H.; Moghaddam, S.H.A.; Naboureh, A.; Ranjgar, B.; et al. Ocean Remote Sensing Techniques and Applications: A Review (Part II). *Water* **2022**, *14*, 3401, doi:10.3390/w14213401.
3. Domingo, M.C. An Overview of the Internet of Underwater Things. *Journal of Network and Computer Applications* **2012**, *35*, 1879–1890, doi:10.1016/j.jnca.2012.07.012.
4. Qiu, T.; Zhao, Z.; Zhang, T.; Chen, C.; Chen, C.L.P. Underwater Internet of Things in Smart Ocean: System Architecture and Open Issues. *IEEE Transactions on Industrial Informatics* **2020**, *16*, 4297–4307, doi:10.1109/TII.2019.2946618.
5. Khalil, R.A.; Saeed, N.; Babar, M.I.; Jan, T. Toward the Internet of Underwater Things: Recent Developments and Future Challenges. *IEEE Consumer Electron. Mag.* **2021**, *10*, 32–37, doi:10.1109/MCE.2020.2988441.
6. Jahanbakht, M.; Xiang, W.; Hanzo, L.; Rahimi Azghadi, M. Internet of Underwater Things and Big Marine Data Analytics—A Comprehensive Survey. *IEEE Commun. Surv. Tutorials* **2021**, *23*, 904–956, doi:10.1109/COMST.2021.3053118.
7. Ayaz, M.; Baig, I.; Abdullah, A.; Faye, I. A Survey on Routing Techniques in Underwater Wireless Sensor Networks. *Journal of Network and Computer Applications* **2011**, *34*, 1908–1927, doi:10.1016/j.jnca.2011.06.009.
8. Ahmed, M.; Salleh, M.; Channa, M.I. Routing Protocols Based on Node Mobility for Underwater Wireless Sensor Network (UWSN): A Survey. *J. Netw. Comput. Appl.* **2017**, *78*, 242–252, doi:10.1016/j.jnca.2016.10.022.
9. Islam, T.; Lee, Y.K. A Comprehensive Survey of Recent Routing Protocols for Underwater Acoustic Sensor Networks. *Sensors* **2019**, *19*, 4256, doi:10.3390/s19194256.
10. Luo, J.; Chen, Y.; Wu, M.; Yang, Y. A Survey of Routing Protocols for Underwater Wireless Sensor Networks. *IEEE Communications Surveys Tutorials* **2021**, *23*, 137–160, doi:10.1109/COMST.2020.3048190.
11. Xie, P.; Zhou, Z.; Nicolaou, N.; See, A.; Cui, J.-H.; Shi, Z. Efficient Vector-Based Forwarding for Underwater Sensor Networks. *J Wireless Com Network* **2010**, *2010*, 1–13, doi:10.1155/2010/195910.
12. Nicolaou, N.; See, A.; Xie, P.; Cui, J.-H.; Maggiorini, D. Improving the Robustness of Location-Based Routing for Underwater Sensor Networks. In Proceedings of the OCEANS 2007 - Europe; June 2007; pp. 1–6.
13. Coutinho, R.W.L.; Boukerche, A.; Vieira, L.F.M.; Loureiro, A.A.F. A Novel Void Node Recovery Paradigm for Long-Term Underwater Sensor Networks. *Ad Hoc Networks* **2015**, *34*, 144–156, doi:10.1016/j.adhoc.2015.01.012.
14. Yan, J.; Zhang, X.; Luo, X.; Wang, Y.; Chen, C.; Guan, X. Asynchronous Localization With Mobility Prediction for Underwater Acoustic Sensor Networks. *IEEE Trans. Veh. Technol.* **2018**, *67*, 2543–2556, doi:10.1109/TVT.2017.2764265.
15. Yan, H.; Shi, Z.J.; Cui, J.-H. DBR: Depth-Based Routing for Underwater Sensor Networks. In Proceedings of the NETWORKING 2008 Ad Hoc and Sensor Networks, Wireless Networks, Next Generation Internet; Das, A., Pung, H.K., Lee, F.B.S., Wong, L.W.C., Eds.; Springer: Berlin, Heidelberg, 2008; pp. 72–86.
16. Wahid, A.; Kim, D. An Energy Efficient Localization-Free Routing Protocol for Underwater Wireless Sensor Networks. *International Journal of Distributed Sensor Networks* **2012**, *8*, 307246, doi:10.1155/2012/307246.

17. Guan, Q.; Ji, F.; Liu, Y.; Yu, H.; Chen, W. Distance-Vector-Based Opportunistic Routing for Underwater Acoustic Sensor Networks. *IEEE Internet of Things Journal* **2019**, *6*, 3831–3839, doi:10.1109/JIOT.2019.2891910.
18. Wang, B.; Zhang, H.; Zhu, Y.; Cai, B.; Guo, X. Adaptive Power-Controlled Depth-Based Routing Protocol for Underwater Wireless Sensor Networks. *JMSE* **2023**, *11*, 1567, doi:10.3390/jmse11081567.
19. Chen, Y.; Zheng, K.; Fang, X.; Wan, L.; Xu, X. QMCR: A Q-Learning-Based Multi-Hop Cooperative Routing Protocol for Underwater Acoustic Sensor Networks. *China Communications* **2021**, *18*, 224–236, doi:10.23919/JCC.2021.08.016.
20. Wu, H.; Chen, X.; Shi, C.; Xiao, Y.; Xu, M. An ACOA-AFSA Fusion Routing Algorithm for Underwater Wireless Sensor Network. *International Journal of Distributed Sensor Networks* **2012**, *8*, 920505, doi:10.1155/2012/920505.
21. Zhou, Y.; Cao, T.; Xiang, W. Anypath Routing Protocol Design via Q-Learning for Underwater Sensor Networks. *IEEE Internet of Things Journal* **2021**, *8*, 8173–8190, doi:10.1109/JIOT.2020.3042901.
22. Zhang, Y.; Zhang, Z.; Chen, L.; Wang, X. Reinforcement Learning-Based Opportunistic Routing Protocol for Underwater Acoustic Sensor Networks. *IEEE Transactions on Vehicular Technology* **2021**, *70*, 2756–2770, doi:10.1109/TVT.2021.3058282.
23. Su, Y.; Fan, R.; Fu, X.; Jin, Z. DQELR: An Adaptive Deep Q-Network-Based Energy- and Latency-Aware Routing Protocol Design for Underwater Acoustic Sensor Networks. *IEEE Access* **2019**, *7*, 9091–9104, doi:10.1109/ACCESS.2019.2891590.
24. Ahmed, S.H.; Lee, S.; Park, J.; Kim, D.; Rawat, D.B. IDFR: Intelligent Directional Flooding-Based Routing Protocols for Underwater Sensor Networks. In Proceedings of the 2017 14th IEEE Annual Consumer Communications & Networking Conference (CCNC); January 2017; pp. 560–565.
25. Stojanovic, M. On the Relationship between Capacity and Distance in an Underwater Acoustic Communication Channel. In Proceedings of the Proceedings of the 1st ACM international workshop on Underwater networks - WUWNet '06; ACM Press: Los Angeles, CA, USA, 2006; p. 41.
26. Freitag, L.; Grund, M.; Singh, S.; Partan, J.; Koski, P.; Ball, K. The WHOI Micro-Modem: An Acoustic Communications and Navigation System for Multiple Platforms. In Proceedings of the Proceedings of OCEANS 2005 MTS/IEEE; September 2005; pp. 1086-1092 Vol. 2.
27. Cortes, C.; Vapnik, V. Support-Vector Networks. *Mach Learn* **1995**, *20*, 273–297, doi:10.1007/BF00994018.
28. Casari, P.; Campagnaro, F.; Dubrovinskaya, E.; Francescon, R.; Dagan, A.; Dahan, S.; Zorzi, M.; Diamant, R. ASUNA: A Topology Data Set for Underwater Network Emulation. *IEEE Journal of Oceanic Engineering* **2021**, *46*, 307–318, doi:10.1109/JOE.2020.2968104.
29. Coutinho, R.W.L.; Boukerche, A.; Vieira, L.F.M.; Loureiro, A.A.F. Geographic and Opportunistic Routing for Underwater Sensor Networks. *IEEE Transactions on Computers* **2016**, *65*, 548–561, doi:10.1109/TC.2015.2423677.
30. Javaid, N.; Hafeez, T.; Wadud, Z.; Alrajeh, N.; Alabed, M.S.; Guizani, N. Establishing a Cooperation-Based and Void Node Avoiding Energy-Efficient Underwater WSN for a Cloud. *IEEE Access* **2017**, *5*, 11582–11593, doi:10.1109/ACCESS.2017.2707531.